

Direct Generation of Airy Beams at Designed Fourier Planes Using Integrated Airy Phase Plates

Dong Wu¹, Xinbo Qi¹, Ze Cai, Dawei Wang¹, Yanlei Hu¹, Jiawen Li¹, and Jiaru Chu

Abstract—Featuring extraordinarily curved propagation trajectories, self-accelerating Airy beams have stimulated considerable interests from academic research to practical applications. However, generation of high-quality Airy beams using compact optical devices is still highly desirable. Here we present a design of integrated Airy phase plates (IAPPs) with a miniature size ($60\ \mu\text{m} \times 60\ \mu\text{m} \times 1.1\ \mu\text{m}$). In addition, a phase-type Fresnel zone plate (FZP) is incorporated in the phase element to further reduce the system dimension, endowing the IAPPs the ability of directly generating Airy beams without introducing a bulky Fourier transform (FT) lens. The fabrication of IAPPs is facilitated by femtosecond direct laser writing (FsDLW), and the experimentally generated Airy beams are in good agreement with the numerical simulations. Furthermore, the flexible fabrication of IAPPs with different focal lengths is demonstrated, which results in the generation of Airy beams at different Fourier planes as desired. Our design strategy and fabrication methodology of the microscale three-dimensional (3D) phase plates can unfold new capacities of Airy beams for miniaturization applications in fiber optics and in on-chip photonics.

Index Terms—Femtosecond laser fabrication, airy beam, integrated optics.

I. INTRODUCTION

THE elegance of physics is once again reflected by the analogy between the mathematical terms of the Schrödinger equation within the context of quantum mechanics and those of the paraxial Helmholtz diffraction equation within the context of optics. In 1979, Berry and Balazs theoretically demonstrated that a free particle can exhibit non-spreading Airy wave packet, which is able to freely accelerate in the absence of an external potential [1]. Nearly three decades later, self-accelerating Airy beams were predicted and experimentally realized in the domain of optics by Siviloglou

and coworkers [2]. Since then, the Airy optical beams have attained enduring research interests due to their intriguing properties including diffraction-free [3], self-healing [4] and quadratic transverse acceleration [5]. By exploiting these features, researchers have widely used optical Airy beams in the fields of microscopy [6] and of optical manipulation [7], in generation of curved plasma channels in air [8] and of femtosecond laser filamentation in water [9], Airy wave bullets [10] and of electron Airy beams [11].

For applications of Airy beams which are in the scale of micrometers, a facile and compact setup which can generate high-quality Airy beams is of vital importance. Up to now, the Airy beam is usually generated by Fourier transforming a Gaussian beam with a cubic phase wavefront. The first observation of optical Airy beams was accomplished by a spatial light modulation (SLM) [3] where cubic phase patterns were encoded. While the intrinsic nature of an SLM with discrete pixels and inactive regions severely limits its ability to yield optical Airy beams with high efficiency. Other attempts such as using Liquid Crystals (LCs) [12], [13], or cylindrical lenses [14], [15] suffer from their bulky dimensions which hindered their applications, in particular, for the integration in miniaturized photonic chips. Recently, metasurfaces has also been developed to form accelerating light with a compact size [16]. However, the preparation of metasurfaces inevitably involves complicated nanofabrication processes and the performance of metasurfaces depends on the polarization of the incident light. As a powerful micromachining technique, femtosecond direct laser writing (FsDLW) has been widely used for the preparation of designed free-form optical elements due to its high precision and flexibility [17], [18]. Micro-optical cubic phase plates have been fabricated by direct laser writing, paving their way to on-chip integration [19]. However, a focusing lens is still needed to perform the Fourier transformation for Airy beams generation (Fig. 1(a)), extending their size to the order of tens of centimeters. Therefore, the development of a low-cost and miniature Airy beam generator is still in high demand.

In this letter, we demonstrate the design and fabrication of integrated Airy phase plates (IAPPs) with a miniature size ($60\ \mu\text{m} \times 60\ \mu\text{m} \times 1.1\ \mu\text{m}$) for directly launching self-accelerating Airy beams without the assistance of an external focusing lens. It is realized by the superposition of the phase of the Fresnel zone plate (FZP) onto the cubic phase plate (Fig. 1(b)). In this way, Airy beams can be generated at the Fourier plane of the phase-type FZP within the length scale of micrometers. The precise adjustment of the generating position

Manuscript received October 19, 2020; revised April 6, 2021; accepted May 4, 2021. Date of publication May 7, 2021; date of current version May 14, 2021. This work was supported in part by the National Natural Science Foundation of China under Grant 51675503, Grant 51875544, and Grant 51805508; in part by the Fundamental Research Funds for the Central Universities under Grant WK2090090012, Grant WK2090000013, and Grant WK2090090021; in part by the Youth Innovation Promotion Association Chinese Academy of Sciences (CAS) under Grant 2017495; and in part by the National Key Research and Development Program of China under Grant 2018YFB1105400. (Corresponding authors: Yanlei Hu; Ze Cai.)

The authors are with the Chinese Academy of Sciences (CAS) Key Laboratory of Mechanical Behavior and Design of Materials, Key Laboratory of Precision Scientific Instrumentation of Anhui Higher Education Institutes, Department of Precision Machinery and Precision Instrumentation, University of Science and Technology of China, Hefei 230027, China (e-mail: huyl@ustc.edu.cn; eilian@mail.ustc.edu.cn).

Color versions of one or more figures in this letter are available at <https://doi.org/10.1109/LPT.2021.3078262>.

Digital Object Identifier 10.1109/LPT.2021.3078262

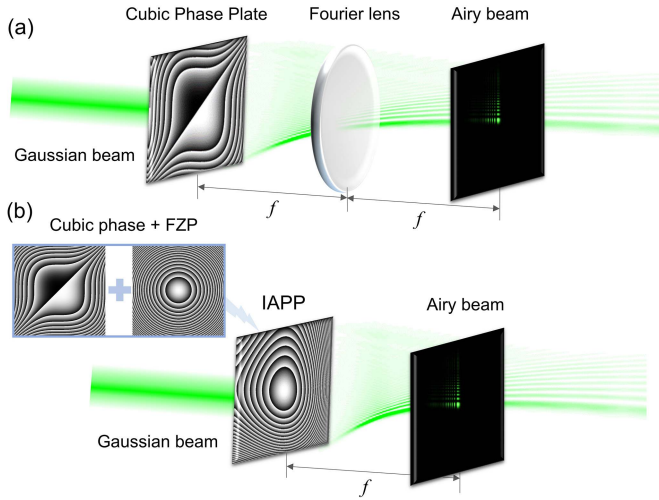


Fig. 1. Schematics of methods for generating Airy beams. (a) Generation of an Airy beam through Fourier transformation of a Gaussian beam imposed with a cubic phase. (b) Direct generation of an Airy beam through the IAPP which is a superposition of the cubic phase and the phase-type FZP.

of Airy beams is facilitated by the excellent depth control of the phase-type FZP. These superiorities are appealing for a wide range of applications such as optical manipulation and photonic microchip integration.

II. DESIGN AND FABRICATION

Our work begins with the envelope of a finite Airy beam, which is the solution of the normalized paraxial equation of diffraction under the condition of introducing an exponential aperture function and could be expressed as:

$$\phi(\xi, s) = Ai \left[s - (\xi/2)^2 + ia\xi \right] \exp[as - (a\xi^2/2) - i(\xi^3/12) + i(a^2\xi/2) + i(s\xi/2)]. \quad (1)$$

$Ai[s - (\xi/2)^2 + ia\xi]$ represents the Airy function, where a is a positive decaying factor to truncate the tail of the infinite Airy beam, and $a \ll 1$. $s = x/x_0$ is a dimensionless transverse coordinate, and x_0 is an arbitrary transverse scale which controls the transversal shift as: $s = (\xi/2)^2$, $\xi = z/kx_0^2$ is a normalized propagation distance and $k = 2\pi n/\lambda$ is the wave number, n is the refractive index of the medium, λ is the free-space wavelength. For the two-dimensional (2D) case, the Fourier spectrum of the Airy beam at the original plane ($\xi = 0$) can be expressed as:

$$\Phi_0(k_x, k_y) \propto \exp \left[-a(k_x^2 + k_y^2) \right] \exp \left[i(k_x^3 + k_y^3)/3 \right]. \quad (2)$$

where k_x and k_y are the Fourier spectrum coordinates.

It indicates that Airy beams can be generated from a Gaussian beam imposed by a cubic phase factor through the Fourier transformation implemented by a Fourier lens (Fig. 1(a)), characterized by a quadratic accelerating trajectory. Then in order to reduce the system dimension, we incorporate the phase information of the cubic phase and of the phase-type FZP ($\varphi(x, y) = -\pi(x^2 + y^2)/\lambda$, where f is the focal length

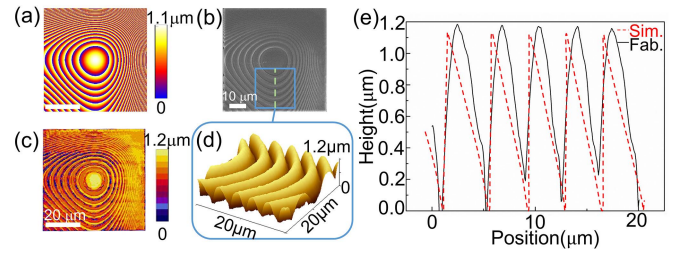


Fig. 2. Characterization of the FsDLW processed IAPP. (a) The designed IAPP with $f = 70 \mu\text{m}$, whose size is $60 \mu\text{m} \times 60 \mu\text{m} \times 1.1 \mu\text{m}$. (b) SEM and (c) Optical profiler images of the fabricated IAPP. (d) AFM image of a local region ($20 \mu\text{m} \times 20 \mu\text{m}$) of the IAPP framed in (b). (e) Height profile of the IAPP along the green dashed line marked in (b), the solid line represents the AFM measured result while the dashed line is the theoretical value.

of the FZP) into one device (Fig. 1(b)) and the Airy beam can be generated at the Fourier plane of the FZP [20].

For the fabrication of IAPPs, the phase information of IAPPs is converted to the height profile which can be precisely controlled by FsDLW. For a material whose refractive index is n_m , the relationship between the phase and the height is:

$$h(x, y) = \lambda\varphi(x, y)/2\pi(n_m - 1). \quad (3)$$

where λ is the free-space wavelength of the incident light which is set to 550 nm here, $\varphi(x, y) = (x^3 + y^3)/3\beta^3 - \pi(x^2 + y^2)/\lambda f$, β is a scale factor which is $6.2 \mu\text{m}$ in this work. Phase discontinuity is introduced by wrapping the phase value with an integer multiple of 2π . The refractive index n_m of the photoresist (SZ2080, provided by IESL-FORTH) mixed with 1 wt.% 4, 4-Bis(diethylamino)benzophenone (BIS) as photoinitiator is ~ 1.5 , so the range of the height is $0 \sim 1100$ nm.

Fig. 2(a) depicts the designed IAPP with $f = 70 \mu\text{m}$, and the size of IAAP is $60 \mu\text{m} \times 60 \mu\text{m} \times 1.1 \mu\text{m}$. A femtosecond laser (Coherent Chameleon Vision-S, 80 MHz repetition rate, 800 nm center wavelength, and 75 fs pulse width) focused by a $60 \times$ oil immersion objective lens (Olympus, NA 1.35) is used to induce two-photon polymerization of the photoresist SZ2080. The fabrication process in the XY plane is controlled by a pair of XY scanning galvo mirrors while the step between two layers in the Z-direction is realized by a nano-positioning stage. Fig. 2(b) shows the scanning electron microscopy (SEM ZEISS EVO18, Germany) image of the fabricated IAPP. To quantitatively characterize the surface morphology, an optical profiler (Contour Elite I, Bruker, Germany) is used to measure the topography of the fabricated IAPP. The surface profile of the fabricated IAPP (Fig. 2(c)) agrees well with the designed one (Fig. 2(a)). To further verify it, a local region of the IAPP is detected by an atomic force microscope (MFP3D-origin OXFORD), as reconstructed in the form of a three-dimensional (3D) image shown in Fig. 2(d). The extracted height profile (Fig. 2(e)) of the IAPP along the green dashed line shown in Fig. 2(b) is consistent with the designed value, guaranteeing the generation of Airy beams as desired. We find a slight mismatch between the designed profile and the experimental results, with a mean absolute error of $0.237 \mu\text{m}$, which is caused by the fabrication error and the subsequent development of the photoresist. This will reduce the quality of the generated Airy beams to some

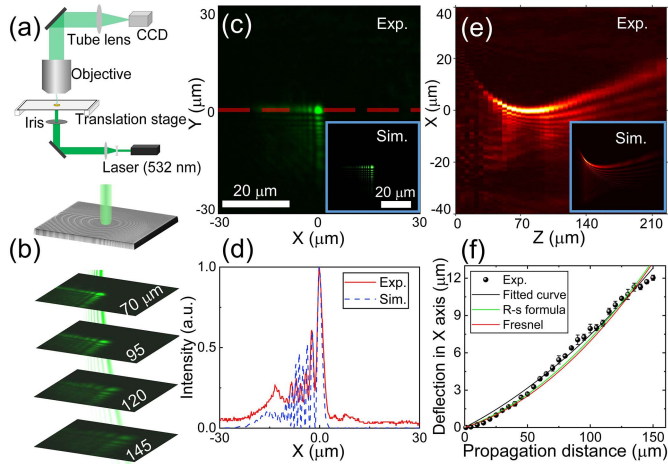


Fig. 3. Direct generation of Airy beams by the fabricated IAPP. (a) Schematics of the experimental setup. (b) Intensity patterns of the Airy beam at propagation planes of $z = 70\mu\text{m}$, $95\mu\text{m}$, $120\mu\text{m}$, $145\mu\text{m}$. (c) Experimental and simulated Airy beam captured at the Fourier plane of the FZP ($70\mu\text{m}$). (d) Normalized intensity profile of the Airy beam along the red dashed line marked in (c). (e) The propagating trajectory of the Airy beam in the X-Z plane. (f) Transverse acceleration of the Airy beam as function of propagation distance from the Fourier plane of the FZP, R-s formula: Rayleigh-Sommerfeld formula.

extent, while from the below experimental characterization of the generated Airy beams, we find this error is within tolerance.

III. MEASUREMENT AND ANALYSIS

Irradiated by a continuous-wave laser beam (532 nm) (Fig. 3(a)), the intensity patterns of the Airy beam can be obtained after the phase plate. A charge-coupled device (CCD) camera is used to capture the light intensity after the magnification of a $40\times$ microscope objective. The fabricated IAPP is fixed on a translation stage and we can acquire the Airy beam dynamics by moving the translation stage along the optical axis. The positions of the translation stage and the CCD are carefully adjusted to make sure the incident condition to be close to normal incident.

Fig. 3(b) demonstrates the intensity patterns of the generated Airy beam at propagation planes of $z = 70\mu\text{m}$, $95\mu\text{m}$, $120\mu\text{m}$, $145\mu\text{m}$. The main lobe of the Airy beam deflects with the propagation distance, which is the most intriguing characteristic of optical Airy beams. Fig. 3(c) shows a more detailed information of Airy beams captured at the Fourier plane of the FZP (i.e., $z = 70\mu\text{m}$). The character of Airy distribution is obvious, which is correspondent with the theoretical simulation (Fig. 3(c) inset). Moreover, the normalized intensity of the Airy beam along the red dashed line shown in Fig. 3(c) is extracted (Fig. 3(d)). The intensity profile of the main lobe of the Airy beam agrees well with the simulated result. As expected, the main lobe occupies the maximum intensity while the Airy tails decay fast. The normalized intensity is not zero between two side lobes, which is caused by the background intensity noise in the region of our fabricated phase plate when we capture the intensity patterns using the CCD camera. To demonstrate the transverse

acceleration, the propagating trajectory of the Airy beam observed along the Y-axis is synthesized (Fig. 3(e)) using the captured light intensity from $z = 0$ to $z = 210\mu\text{m}$. The inset in Fig. 3(e) shows the simulated propagation trajectory. Both the experimental trajectory and the simulated result show a strong beam deflection and match well. The transverse deflection of the Airy beam starting from the Fourier plane of the FZP (i.e., $z = 70\mu\text{m}$) is investigated (Fig. 3(f)) (the black fitted curve). Firstly, we use Fresnel diffraction formula to simulate the propagation trajectory of the Airy beam as this integration method of the IAPP is based on the Fresnel diffraction theory. The simulated result (the red line) agrees well with the experimental result except for a small difference, which is introduced by the fabrication and measurement errors. The use of a quadratic function to fit the experimental results may introduce another error factor because the existence of the additional square phase term [21] in the Fourier plane of the IAPPs makes the trajectory of the beam no longer a strictly parabola trajectory. We emphasize that because the size of the IAPP is not small enough compared to the propagation distance, the Rayleigh-Sommerfeld diffraction theory is more suitable, which is proved by the simulated result. As shown in Fig. 3(f), although these two kinds of diffraction theory are both agreed well with the experimental result, the fitted curve calculated by the Rayleigh-Sommerfeld formula is closer to the experimental result.

The excellent depth control by the FZP is another advantage of our method. For the traditional method (Fig. 1(a)), the adjustment of the generation plane of Airy beams requires the replacement of the Fourier lens which greatly increases the expense of the readjustment. While with the introduction of the phase-type FZPs, Airy beams can be obtained at the corresponding focal planes of the FZPs as desired. Benefited from the high flexibility of the FsDLW methodology, IAPPs with different parameters can be facily fabricated in the same manner. We designed and fabricated four different IAPPs with $f = 50\mu\text{m}$, $60\mu\text{m}$, $80\mu\text{m}$, $90\mu\text{m}$ (Fig. 4(a)). The intensity patterns of the Airy beams generated at the corresponding Fourier planes (Fig. 4(b)) display different distributions resulting from the corresponding focal lengths. Fig. 4(c) shows the deflection profiles of these Airy beams in the X-direction after the corresponding Fourier planes. The solid lines are the fitted curves of the experimental results of the Airy beams with $f = 50\mu\text{m}$, $60\mu\text{m}$, $70\mu\text{m}$, $80\mu\text{m}$, $90\mu\text{m}$, respectively, and the dashed lines are the corresponding simulated results calculated by the Rayleigh-Sommerfeld formula. It is demonstrated that shortening of focal length f results in a higher transverse deflection. All of the experimental results are in good agreement with the simulated trajectories. The high flexibility of FsDLW can also help with the integration of IAPPs on a high-aspect-ratio structure such as an optical fiber. The SEM images in Figs. 4(d)-(e) show the integration of the IAPP with $f = 70\mu\text{m}$ on a single-mode optical fiber facet, and for a simple demonstration, the generated Airy beam under a white light illumination is shown in Fig. 4(f). It proves that the proposed IAPPs have a high level of integration, which can find applications in integrated optics and micro-optical devices.

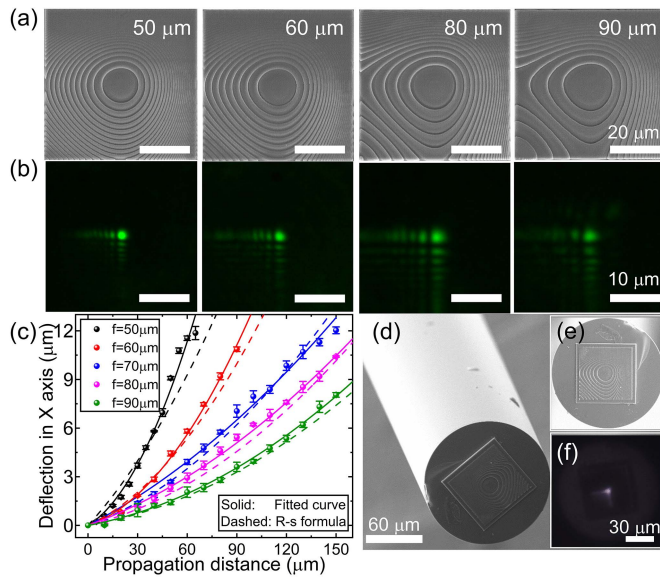


Fig. 4. Flexible fabrication of IAPPs with different focal lengths and the integration of the IAPP on an optical fiber facet. (a) SEM images of the fabricated IAPPs with $f = 50\mu\text{m}, 60\mu\text{m}, 80\mu\text{m}, 90\mu\text{m}$, respectively. (b) Intensity distributions of the Airy beams generated at the corresponding Fourier planes. (c) The deflection profiles of Airy beams generated by IAPPs with different focal lengths. (d-e) 45° tilted and top-view SEM micrographs of the IAPP with $f = 70\mu\text{m}$ fabricated on a single-mode optical fiber facet. (f) The Airy beam generated by the integrated IAPP at a distance of $70\mu\text{m}$ behind the IAPP under a white light illumination.

IV. CONCLUSION

In conclusion, the design and fabrication of integrated Airy phase plates are proposed. The miniature IAPPs are realized by exquisitely incorporating the cubic phase and the phase-type FZP. The IAPPs with different parameters are fabricated by controllable FsDLW with a high surface quality, showcasing the flexibility and precision of this 3D fabrication methodology. The intriguing transverse self-accelerating characteristics of the generated Airy beams are experimentally demonstrated, which are in good agreement with the simulated results. Our fabricated IAPPs have a micrometer dimension, moreover, the incorporation of the phase-type FZP further increases the levels of integration, which is essential for some cases that one wants to integrate the phase plate into microscale optical elements (e.g., fabrication of the phase plate on an optical fiber). This ultra-compact IAPPs hold great promises in the applications of optical manipulation, fiber optics and on-chip photonics.

ACKNOWLEDGMENT

The authors acknowledge the Experimental Center of Engineering and Material Sciences at USTC for the fabrication and measuring of samples. This work was partly carried out

at the USTC Center for Micro and Nanoscale Research and Fabrication.

REFERENCES

- [1] M. V. Berry and N. L. Balazs, "Nonspreading wave packets," *Amer. J. Phys.*, vol. 47, no. 3, pp. 264–267, Mar. 1979.
- [2] G. A. Siviloglou and D. N. Christodoulides, "Accelerating finite energy Airy beams," *Opt. Lett.*, vol. 32, no. 8, pp. 979–981, Apr. 2007.
- [3] G. A. Siviloglou, J. Broky, A. Dogariu, and D. N. Christodoulides, "Observation of accelerating airy beams," *Phys. Rev. Lett.*, vol. 99, no. 21, Nov. 2007, Art. no. 213901.
- [4] J. Broky, G. A. Siviloglou, A. Dogariu, and D. N. Christodoulides, "Self-healing properties of optical Airy beams," *Opt. Exp.*, vol. 16, no. 17, pp. 12880–12891, Aug. 2008.
- [5] G. A. Siviloglou, J. Broky, A. Dogariu, and D. N. Christodoulides, "Ballistic dynamics of Airy beams," *Opt. Lett.*, vol. 33, no. 3, pp. 207–209, Feb. 2008.
- [6] T. Vetteng et al., "Light-sheet microscopy using an airy beam," *Nature Methods*, vol. 11, no. 5, pp. 541–544, May 2014.
- [7] S. Jia, J. C. Vaughan, and X. Zhuang, "Isotropic three-dimensional super-resolution imaging with a self-bending point spread function," *Nature Photon.*, vol. 8, no. 4, pp. 302–306, Apr. 2014.
- [8] P. Polynkin, M. Kolesik, J. V. Moloney, G. A. Siviloglou, and D. N. Christodoulides, "Curved plasma channel generation using ultraintense airy beams," *Science*, vol. 324, no. 5924, pp. 229–232, Apr. 2009.
- [9] P. Polynkin, M. Kolesik, and J. Moloney, "Filamentation of femtosecond laser Airy beams in water," *Phys. Rev. Lett.*, vol. 103, no. 12, Sep. 2009, Art. no. 123902.
- [10] A. Chong, W. H. Renninger, D. N. Christodoulides, and F. W. Wise, "Airy–Bessel wave packets as versatile linear light bullets," *Nature Photon.*, vol. 4, no. 2, pp. 103–106, Jan. 2010.
- [11] N. Voloch-Bloch, Y. Lereah, Y. Lilach, A. Gover, and A. Arie, "Generation of electron airy beams," *Nature*, vol. 494, no. 7437, pp. 331–335, Feb. 2013.
- [12] H. T. Dai, X. W. Sun, D. Luo, and Y. J. Liu, "Airy beams generated by a binary phase element made of polymer-dispersed liquid crystals," *Opt. Exp.*, vol. 17, no. 22, pp. 19365–19370, Oct. 2009.
- [13] D. Luo, H. T. Dai, and X. W. Sun, "Polarization-independent electrically tunable/switchable Airy beam based on polymerstabilized blue phase liquid crystal," *Opt. Exp.*, vol. 21, no. 25, pp. 31318–31323, Dec. 2013.
- [14] D. G. Papazoglou, S. Suntsov, D. Abdollahpour, and S. Tzortzakis, "Tunable intense airy beams and tailored femtosecond laser filaments," *Phys. Rev. A, Gen. Phys.*, vol. 81, no. 6, Jun. 2010, Art. no. 061807.
- [15] A. Valdmann, P. Piksarv, H. Valtna-Lukner, and P. Saari, "Realization of laterally nondispersing ultrabroadband Airy pulses," *Opt. Lett.*, vol. 39, no. 7, pp. 1877–1880, Apr. 2014.
- [16] Q. Fan et al., "Broadband generation of photonic spin-controlled arbitrary accelerating light beams in the visible," *Nano Lett.*, vol. 19, no. 2, pp. 1158–1165, Feb. 2019.
- [17] T. Gissibl, S. Thiele, A. Herkommer, and H. Giessen, "Two-photon direct laser writing of ultracompact multi-lens objectives," *Nature Photon.*, vol. 10, no. 8, pp. 554–560, Aug. 2016.
- [18] L. Jiang et al., "Performance comparison of acrylic and thiol-acrylic resins in two-photon polymerization," *Opt. Exp.*, vol. 24, no. 12, pp. 13687–13701, Jun. 2016.
- [19] Z. Cai et al., "Continuous cubic phase microplates for generating high-quality Airy beams with strong deflection," *Opt. Lett.*, vol. 42, no. 13, pp. 2483–2486, Jul. 2017.
- [20] Q. Lu, S.-J. Gao, Y.-X. Ni, J.-B. Wu, and Y.-F. Qiao, "Generation of airy beams using a phase-only fresnel holographic lens," *Optoelectron. Lett.*, vol. 13, no. 3, pp. 197–200, May 2017.
- [21] J. Ling, Q. Yang, S. Zhang, Q. Lu, S. Liu, and C. Guo, "Improved generation method utilizing a modified Fourier spectrum for Airy beams with the phase-only filter technique," *Appl. Opt.*, vol. 56, no. 25, pp. 7059–7066, Sep. 2017.